On the efficient evaluation of integrals arising in the Sommerfeld halfspace problem

K.A. Michalski, Ph.D.

Indexing terms: *Mathematical techniques, Antennas*

Abstract: An efficient approach is described for the numerical evaluation of the Sommerfeld integrals which arise in analyses of antennas radiating over a dielectric halfspace. The main features of this approach can be summarised as follows. The contour deformation principle is employed to express the original integral as a sum of the steepest descent-path (SDP) integral and the possible branch-cut-path (BCP) integral, which are then evaluated numerically. If the branch point is captured, the SDP is allowed to go to the bottom sheet of the Riemann surface, resulting in a continuous behaviour of the integrand. In the last case, the BCP is deformed to the SDP emanating from the branch point, on which the integrand decays rapidly. Also, the Zenneck pole is subtracted, resulting in a smooth behaviour of the integrand on the SDP.

1 Introduction

A variety of methods exist for the evaluation of the integrals arising in the Sommerfeld halfspace problem [1]. For a comprehensive summary of these techniques, the reader is referred to the recent review papers [2–4]. These techniques can roughly be classified as analytic or numerical. The analytic methods are based on approximations, which inevitably apply for only a limited range of parameters. The numerical techniques are usually 'exact' in the sense that a numerical quadrature is applied to rigorous Sommerfeld integrals. These techniques, too, are only applicable in some range of parameters outside which the computational cost becomes prohibitive. Therefore, efforts continue to develop new, more efficient and more widely applicable methods for the evaluation of Sommerfeld integrals. The papers by Rahmat-Samii *et al.* [2, 5], Johnson and Dudley [6], and Lindell and Alanen [7] are examples of the more recent developments in this field.

The present paper elaborates upon the Rahmat-Samii *et al.* technique for the computation of the Sommerfeld integrals which arise in analyses of antennas radiating over a dielectric halfspace. In contrast to previous approaches [3], these authors deform the original path of integration to the steepest descent path (SDP) passing through the saddle point, as it is done in the asymptotic approximation of integrals [8, 9]. The Sommerfeld integral is then evaluated numerically along the SDP. It is quite obvious that this choice of the path of integration is superior to other approaches in the case when the distance between the source point and the observation point is large in terms of wavelengths. Rahmat-Samii *et al.* have found, however, that the integration along the SDP is very efficient even if the last condition is drastically violated. This surprising observation is the key to the success of their technique.

A complication in the Rahmat-Samii *et al.* method arises when a branch point is captured in the process of the contour deformation. In that case, in order to remain on the top sheet of the Riemann surface, the branch-cut-path (BCP) integral is added to the SDP integral. The BCP integral is only along the part of the fundamental branch cut which is captured by the SDP. This treatment of the branch point singularity has several disadvantages which can adversely affect the efficiency of the overall scheme. First, due to the fact that the SDP is kept on the top sheet, the integrand exhibits a discontinuity at the point where the SDP crosses the branch cut, which necessitates splitting the integration interval in two. Secondly, the limit of integration in the BCP integral must be found as a solution of a nonlinear equation, which is a rather unreliable process. Finally, the integrand along the BCP often varies rapidly, requiring a high-order quadrature.

Another difficulty in this scheme is due to the pole of the integrand (the Zenneck pole [8]), which, although never captured, can get arbitrarily close to the SDP when both the source point and the field point are close to the interface and the contrast between the two media is large. In that case, the integrand exhibits a sharp peak on the SDP in the vicinity of the pole, requiring a very careful integration.

In this paper, a modification of the Rahmat-Samii *et al.* approach is described, which does not suffer from the deficiencies stated above. The main features of the modified technique can be summarised as follows. If the branch point is captured, the SDP is allowed to go to the bottom sheet of the Riemann surface, resulting in a continuous behaviour of the integrand. To properly close the contour of integration, the SDP integral is augmented by an integral around the entire branch cut. The original branch cut is then deformed to the SDP emanating from the branch point, on which the integrand decays rapidly. Finally, the Zenneck pole is subtracted from the integrand along the SDP, making the integration efficient and reliable for a wide range of parameters. The integral of the subtracted term is then expressed in terms of the error function and is added to the modified integral to preserve its correct value.

2 Formulation

Consider a vertical electric dipole (VED) of unit strength located at height h above a planar interface separating two halfspaces (Fig. 1). The medium of the upper halfspace ($z > 0$) is taken to be air with permittivity ε_0, permeability μ_0 and wave number k_1. The lower halfspace ($z < 0$) is occupied by a dielectric characterised by ($\kappa\varepsilon_0$, μ_0) with $\kappa = \varepsilon - j\sigma/(\omega\varepsilon_0)$, where ε is the relative dielectric constant and σ is the conductivity of the medium (the exp ($j\omega t$) time convention is assumed). The Hertz vector due to the VED is given by $\Pi_v = \hat{z}\Pi_{vz}$, where $\hat{z}$ is a unit vector in the z-direction, and where Π_{vz} can be expressed as [2]

$$\Pi_{vz} = (j\omega\varepsilon_0)^{-1}\{g(r_1) - g(r_2) + {}_0\Pi_{vz}\} \quad (1)$$

Paper 3965H (E11), received 13th July 1985

The author is with the Department of Electrical Engineering, University of Mississippi, Mississippi 38677, USA

with

$$g(r) = \exp(-jk_1 r)/4\pi r \tag{2}$$

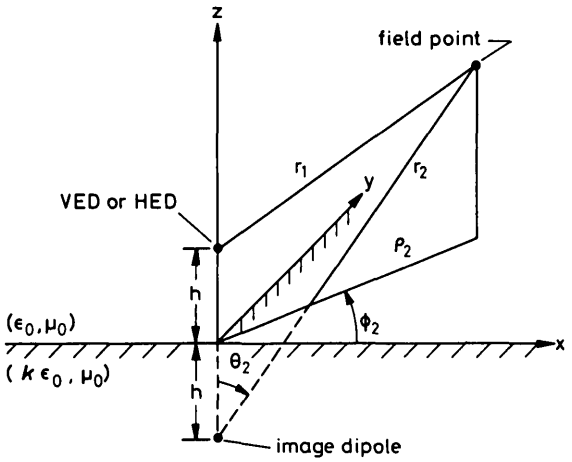

Fig. 1 *Elementary dipole radiating over a dielectric halfspace*

and

$${}_0\Pi_{vz} = \frac{k_1\kappa}{4\pi j}\int_\Gamma \frac{\sin\xi\cos\xi}{\kappa\cos\xi + \sqrt{\kappa - \sin^2\xi}} \times H_0^{(2)}(k_1\rho_2\sin\xi)e^{-jk_1(z+h)\cos\xi}\,d\xi \tag{3}$$

In eqn. 3, $H_0^{(2)}$ is the Hankel function of the second kind and order zero, and Γ is the path of integration on the top sheet of the two-sheeted Riemann surface (Fig. 2). The top

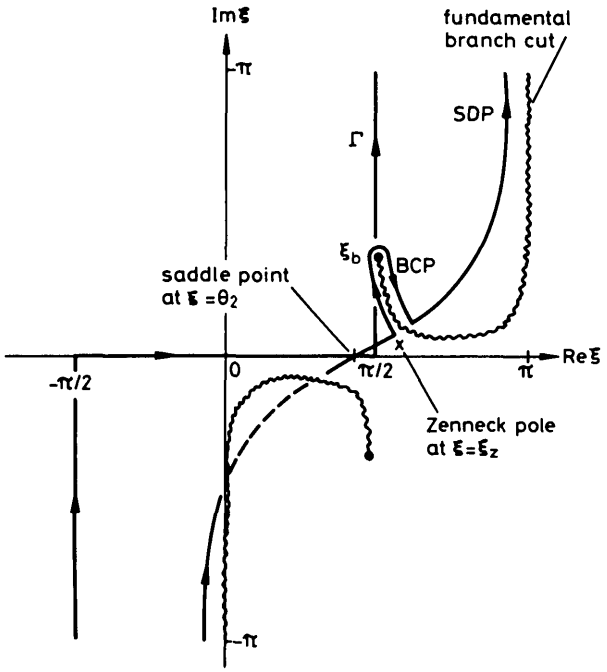

Fig. 2 *The original integration path Γ, the steepest-descent path (SDP), and the branch-cut path (BCP) in the complex ξ-plane*
$f = 10$ Mhz, $\varepsilon = 10$, $\sigma = 2 \cdot 10^{-4}$ S/m, and $\theta_2 = 78°$

and bottom sheets are defined by

$$\text{Im}\{\sqrt{\kappa - \sin^2\xi}\}\begin{cases} <0, \text{ on top sheet} & (4a)\\ =0, \text{ on fundamental branch cuts} & (4b)\\ >0, \text{ on bottom sheet} & (4c)\end{cases}$$

When the VED is replaced by a horizontal electric dipole (HED), which without loss of generality can be assumed to be along the x-axis, the Hertz vector is given by $\Pi_h = \hat{x}\Pi_{hx} + \hat{z}\Pi_{hz}$ where Π_{hx} and Π_{hz} can be expressed as [2, 5]

$$\Pi_{hx} = (j\omega\varepsilon_0)^{-1}\{g(r_1) - g(r_2) + {}_0\Pi_{hx}\} \tag{5}$$

$$\Pi_{hz} = (j\omega\varepsilon_0)^{-1}{}_0\Pi_{hz} \tag{6}$$

with

$${}_0\Pi_{hx} = \frac{k_1}{4\pi j}\int_\Gamma \frac{\sin\xi\cos\xi}{\cos\xi + \sqrt{\kappa - \sin^2\xi}} \times H_0^{(2)}(k_1\rho_2\sin\xi)e^{-jk_1(z+h)\cos\xi}\,d\xi \tag{7}$$

and

$${}_0\Pi_{hz} = -\frac{k_1}{4\pi}\cos\phi_2\int_\Gamma \sin^2\xi\cos\xi\,\frac{\cos\xi - \sqrt{\kappa - \sin^2\xi}}{\kappa\cos\xi + \sqrt{\kappa - \sin^2\xi}} \cdot H_1^{(2)}(k_1\rho_2\sin\xi)e^{-jk_1(z+h)\cos\xi}\,d\xi \tag{8}$$

It is worth mentioning, before leaving this Section, that there are other ways of expressing Π_{vz} and Π_{hx} than given above. For example, eqn. 1 can be rewritten as

$$\Pi_{vz} = (j\omega\varepsilon_0)^{-1}\{g(r_1) + g(r_2) + {}_0\Pi'_{vz}\} \tag{9}$$

with

$${}_0\Pi'_{vz} = -\frac{k_1}{4\pi j}\int_\Gamma \frac{\sin\xi\sqrt{\kappa - \sin^2\xi}}{\kappa\cos\xi + \sqrt{\kappa - \sin^2\xi}} \times H_0^{(2)}(k_1\rho_2\sin\xi)e^{-jk_1(z+h)\cos\xi}\,d\xi \tag{10}$$

When the lower medium is replaced by a perfect conductor, Π_{vz} and Π_{hx} are given by the first two terms of eqns. 9 and 5, respectively (Π_{hz} is zero in that case). Although eqn. 9 is more consistent with eqn. 5, the representation, eqn. 1, is used throughout this paper, as it was employed in the original formulation [2].

The remainder of this paper is concerned with the evaluation of the integrals incorporated in ${}_0\Pi_{vz}$, ${}_0\Pi_{hx}$, and ${}_0\Pi_{hz}$, which are known as the Sommerfeld integrals. The integral contained in ${}_0\Pi_{vz}$ is used in the numerical examples included in the next Sections, as it incorporates all the important features of all the Sommerfeld integrals.

3 Evaluation of the Sommerfeld integrals [2, 5]

Rahmat-Samii *et al.* evaluate the Sommerfeld integrals incorporated in eqns. 3 and 7–8 by deforming Γ to the steepest descent path (SDP) in the complex ξ-plane (Fig. 2) and by making the substitution

$$\cos(\xi - \theta_2) = 1 - js^2 \tag{11}$$

where s is a real variable ranging between $-\infty$ and $+\infty$, with $s = 0$ corresponding to the saddle point at $\xi = \theta_2$. From eqn. 11, the SDP is given by [2, 5]

$$\xi_{SDP} = \theta_2 - j\,\text{Ln}\left((1 - js^2) - s(1 - j)\sqrt{1 - j\frac{s^2}{2}}\right) \tag{12}$$

In deforming Γ to the SDP, the branch point $\xi_b = \xi'_b + j\xi''_b$ can be captured, which occurs when $\theta_2 > \theta_c$, where θ_c is the angle of capture given by [8]

$$\theta_c = \xi'_b - \arccos\left(\frac{1}{\cosh(\xi''_b)}\right) \tag{13}$$

with

$$\xi_b = \frac{\pi}{2} + j\,\text{Ln}(\sqrt{\kappa} + \sqrt{\kappa - 1}) \tag{14}$$

When this happens, the contour of integration must be properly modified to take into account the branch-cut contribution. Rahmat-Samii *et al.* let the SDP enter the

bottom sheet when it crosses the lower branch cut (Fig. 2), as it always re-emerges on the top sheet. However, they do not allow the SDP to go to the bottom sheet when it encounters the upper branch cut and integrate around it instead. The path around the captured part of the branch cut is designated BCP in Fig. 2.

Invoking the unit step function

$$u(x) = \begin{cases} 1, & x > 0 \\ 0, & x < 0 \end{cases} \tag{15}$$

one can express each of the Hertz potentials as a sum of the SDP contribution, and the possible BCP contribution as

$${}_0\Pi_{vz} = {}_0\Pi_{vz}^{SDP} + u(\theta - \theta_c){}_0\Pi_{vz}^{BCP} \tag{16}$$

$${}_0\Pi_{hx} = {}_0\Pi_{hx}^{SDP} + u(\theta - \theta_c){}_0\Pi_{hx}^{BCP} \tag{17}$$

$${}_0\Pi_{hz} = {}_0\Pi_{hz}^{SDP} + u(\theta - \theta_c){}_0\Pi_{hz}^{BCP} \tag{18}$$

The SDP terms in eqns. 16–18 are given by

$${}_0\Pi_{vz}^{SDP} = \frac{k_1\kappa}{4\pi j} e^{-jk_1r_2} \int_{-\infty}^{\infty} P(\xi_{SDP})\alpha(s)e^{-k_1r_2s^2}\, ds \tag{19}$$

$${}_0\Pi_{hx}^{SDP} = \frac{k_1}{4\pi j} e^{-jk_1r_2} \int_{-\infty}^{\infty} S(\xi_{SDP})\alpha(s)e^{-k_1r_2s^2}\, ds \tag{20}$$

and

$${}_0\Pi_{hz}^{SDP} = -\frac{k_1}{4\pi} \cos\phi_2\, e^{-jk_1r_2} \times \int_{-\infty}^{\infty} T(\xi_{SDP})\alpha(s)e^{-k_1r_2s^2}\, ds \tag{21}$$

where

$$P(\xi) = \frac{1}{\kappa\cos\xi + \sqrt{\kappa - \sin^2\xi}} Q_0(\xi) \tag{22}$$

$$S(\xi) = \frac{1}{\cos\xi + \sqrt{\kappa - \sin^2\xi}} Q_0(\xi) \tag{23}$$

$$T(\xi) = \sin\xi \frac{\cos\xi - \sqrt{\kappa - \sin^2\xi}}{\kappa\cos\xi + \sqrt{\kappa - \sin^2\xi}} Q_1(\xi) \tag{24}$$

with

$$Q_i(\xi) = \sin\xi\cos\xi H_i^{(2)}(k_1r_2\sin\theta_2\sin\xi) \times e^{jk_1r_2\sin\theta_2\sin\xi} \quad i = 0, 1 \tag{25}$$

and where

$$\alpha(s) \equiv \frac{d\xi}{ds} = \frac{1+j}{\sqrt{1 - j\frac{s^2}{2}}} \tag{26}$$

The condition 4*a* is enforced along the SDP in eqns. 22–24, except for the part of the path which is on the bottom sheet (denoted by a dashed line in Fig. 2), where condition 4*c* holds. The effective interval of integration is determined from the condition [2]

$$|s| \leqslant \frac{3}{\sqrt{k_1r_2}} \tag{27}$$

As an illustration of the typical behaviour of the Sommerfeld integrands, the integrand of ${}_0\Pi_{vz}^{SDP}$ is plotted for two different sets of parameters in Figs. 3*a* and 4*a*. These examples show the undesirable discontinuity of the integrands at the point where the SDP crosses the upper branch cut.

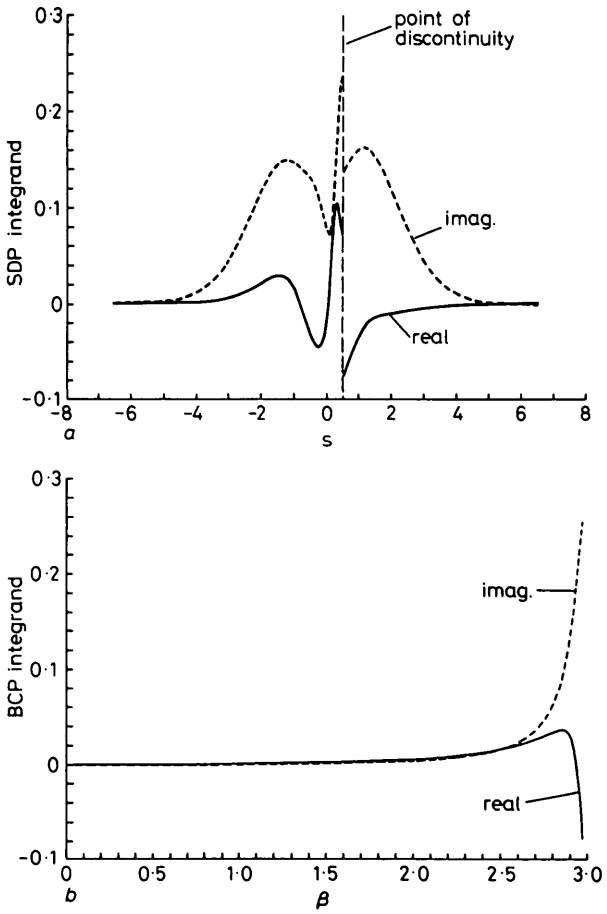

Fig. 3 *Plot of the ${}_0\Pi_{vz}$ integrand (Rahmat-Samii et al. [2, 5] approach)*
$f = 10$ MHz, $\varepsilon = 10$, $\sigma = 2 \cdot 10^{-4}$ S/m, $\theta_2 = 78°$, and $r_2 = 1$ m
a SDP integrand *b* BCP integrand

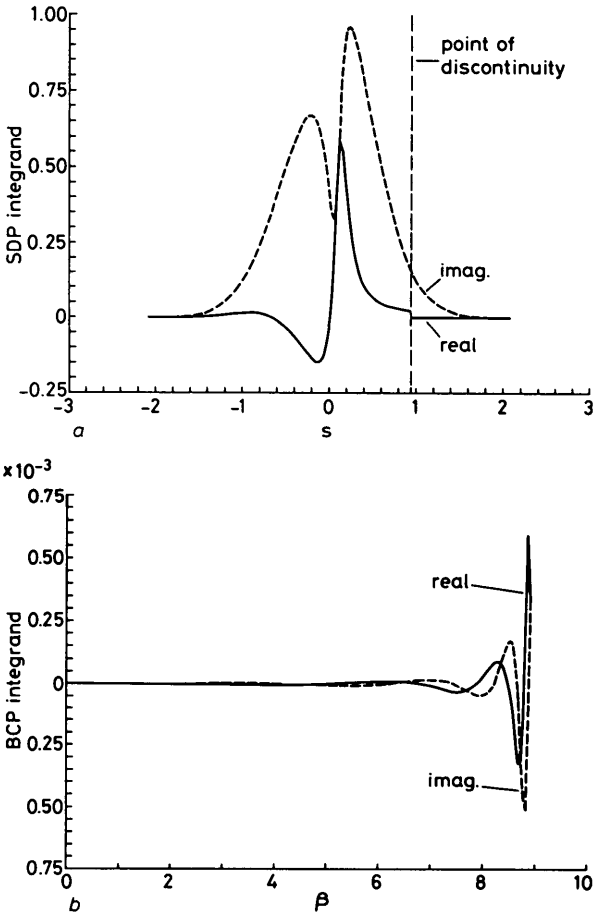

Fig. 4 *Plot of the ${}_0\Pi_{vz}$ integrand (Rahmat-Samii et al. [2, 5] approach)*
$f = 100$ MHz, $\varepsilon = 80$, $\sigma = 1 \cdot 10^{-2}$ S/m, $\theta_2 = 85°$, and $r_2 = 1$ m
a SDP integrand *b* BCP integrand

The BCP terms in eqns. 16–18 contain integrals around the captured part of the fundamental branch cut. Rahmat-Samii *et al.* express these integrals in terms of a real parameter β ranging between zero and some finite value β_1, which must be determined as a solution of a nonlinear equation. For more details, the reader is referred to References 2 and 5. To illustrate the typical behaviour of the integrands along the fundamental branch cut, the integrand of ${}_0\Pi_{vz}^{BCP}$ is plotted in Figs. 3*b* and 4*b* for the two cases. One observes a rapid variation of the integrands near the end of the interval, which necessitates a very careful integration.

4 Improved method

The discontinuity of the SDP integrand in the Rahmat-Samii *et al.* approach can be removed if one allows the SDP to continue on the bottom sheet when it encounters the upper fundamental branch cut. However, since the original path Γ must meet with the deformed contour on the same sheet at infinity, the SDP integral must be augmented in that case by an integral around the entire branch cut, as illustrated in Fig. 5*a*. Obviously, the necessity to integrate along this contour would nullify any gain of efficiency in the SDP integral. To remedy this, the fundamental branch cut is deformed to the steepest descent path from the branch point ξ_b (Fig. 5*b*), as is done in the asymptotic evaluation of branch-cut integrals [8, 9]. This is accomplished by making the substitution

$$\cos(\xi - \theta_2) = \cos(\xi_b - \theta_2) - jt^2 \tag{28}$$

where t is a real parameter ranging between $-\infty$ and $+\infty$. From eqn. 28, the deformed branch cut can be explicitly defined as

$$\xi_{BCP} = \theta_2 - j\,\mathrm{Ln}\,(\cos(\xi_b - \theta_2) - jt^2 + j\sqrt{t^4 + j2t^2\cos(\xi_b - \theta_2) + \sin^2(\xi_b - \theta_2)}) \tag{29}$$

No singularities are captured in the BCP deformation since the pole ξ_z (the Zenneck pole [8, 9]) exhibited by $P(\xi)$ and $T(\xi)$ lies below the original branch cut [9].

When eqn. 28 is used in eqns. 3 and 7–8, the BCP terms in eqns. 16–18 can be expressed as

$${}_0\Pi_{vz}^{BCP} = \frac{k_1\kappa}{4\pi j}\, e^{-jk_1r_2\cos(\xi_b-\theta_2)} \times \int_0^\infty P'(\xi_{BCP})\beta(t)e^{-k_1r_2t^2}\,dt \tag{30}$$

$${}_0\Pi_{hx}^{BCP} = \frac{k_1}{4\pi j}\, e^{-jk_1r_2\cos(\xi_b-\theta_2)} \times \int_0^\infty S'(\xi_{BCP})\beta(t)e^{-k_1r_2t^2}\,dt \tag{31}$$

and

$${}_0\Pi_{hz}^{BCP} = -\frac{k_1}{4\pi}\cos\phi_2\, e^{-jk_1r_2\cos(\xi_b-\theta_2)} \times \int_0^\infty T'(\xi_{BCP})\beta(t)e^{-k_1r_2t^2}\,dt \tag{32}$$

where

$$P'(\xi) = P^-(\xi) - P^+(\xi) = \frac{2\sqrt{\kappa - \sin^2\xi}}{(\kappa-1)[(\kappa+1)\cos^2\xi - 1]}\,Q_0(\xi) \tag{33}$$

$$S'(\xi) = S^-(\xi) - S^+(\xi) = -\frac{2\sqrt{\kappa - \sin^2\xi}}{(\kappa-1)}\,Q_0(\xi) \tag{34}$$

$$T'(\xi) = T^-(\xi) - T^+(\xi) = \frac{2(\kappa+1)\sqrt{\kappa - \sin^2\xi}}{(\kappa-1)[(\kappa+1)\cos^2\xi - 1]}\sin\xi\cos\xi Q_1(\xi) \tag{35}$$

and where

$$\beta(t) \equiv \frac{d\xi}{dt} = \frac{j2t}{\sqrt{1 - [\cos(\xi_b - \theta_2) - jt^2]^2}} \tag{36}$$

The minus or plus superscripts in the integrands in eqns. 33–35 signify that the branch of the square root is chosen

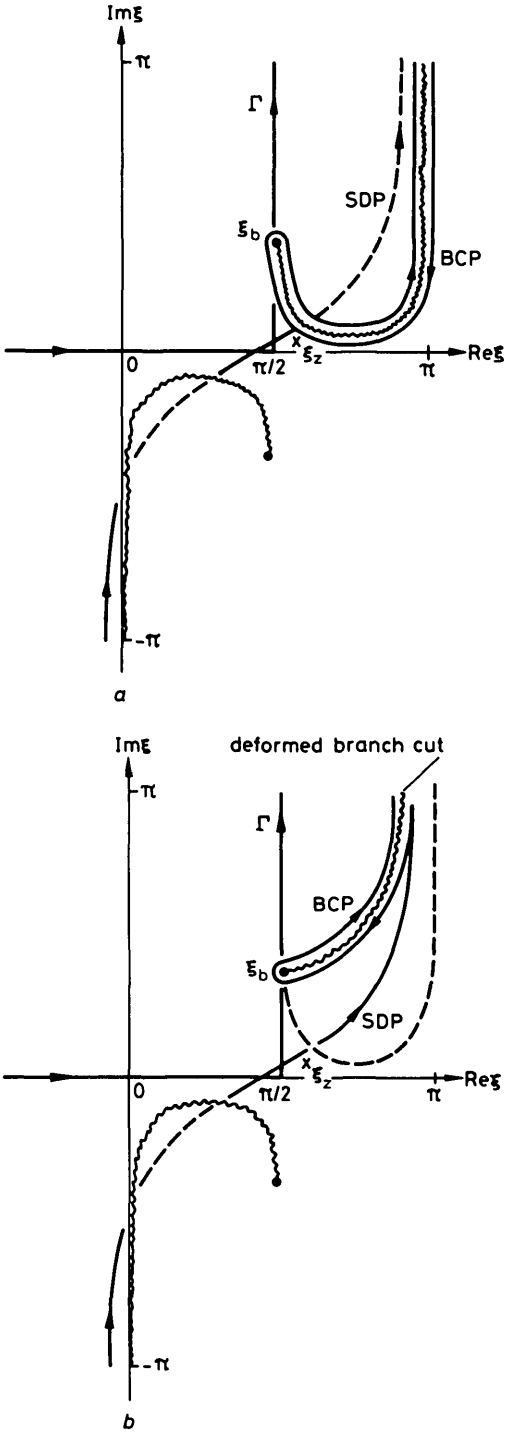

Fig. 5 *Proposed integration paths in the complex ξ-plane*
$f = 10$ MHz, $\varepsilon = 10$, $\sigma = 2.10^{-4}$ S/m, and $\theta_2 = 78°$
a Before branch-cut deformation
b After branch-cut deformation to the steepest-descent path from the branch point

according to eqn. 4*a* or 4*c*, respectively. The effective limits of integration in eqns. 30–32 are determined by the criterion, eqn. 27.

To illustrate the behaviour of the integrands in the modified method, the integrands of ${}_0\Pi_{vz}^{SDP}$ and ${}_0\Pi_{vz}^{BCP}$ are plotted in Figs. 6 and 7 for the cases of Figs. 3 and 4. It is

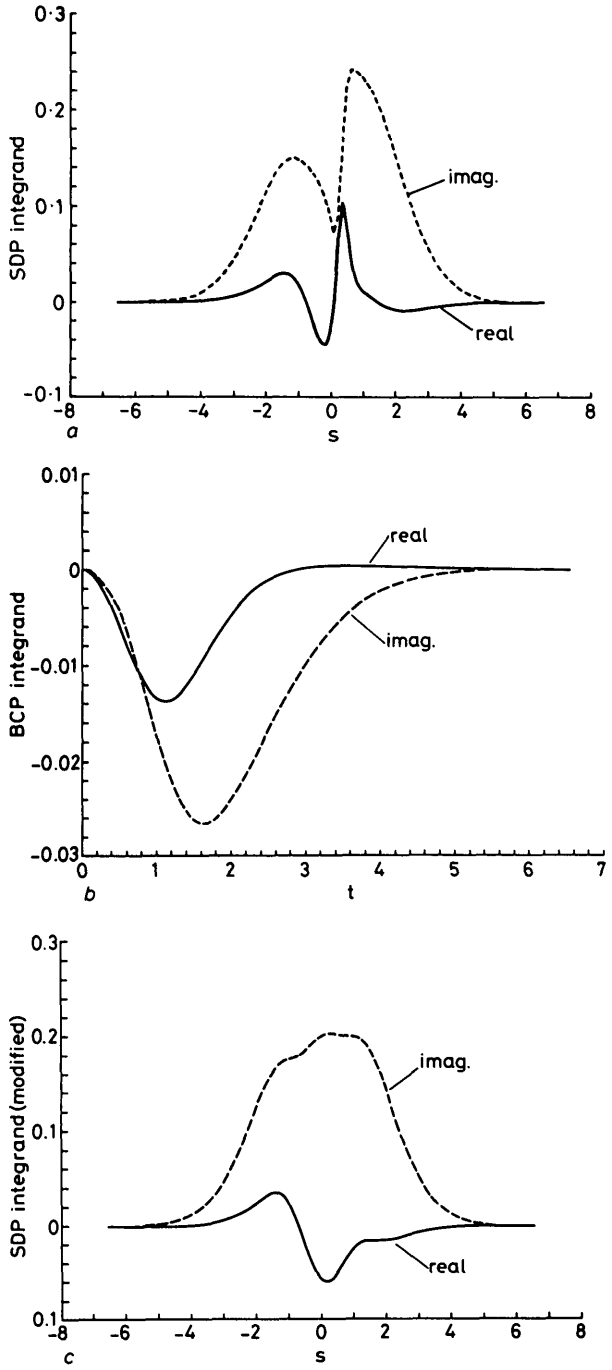

Fig. 6 *Plot of the* ${}_0\Pi_{vz}$ *integrand (improved approach) for the parameters of Fig. 3*

a SDP integrand
b BCP integrand
c Modified SDP integrand (Zenneck pole subtracted)

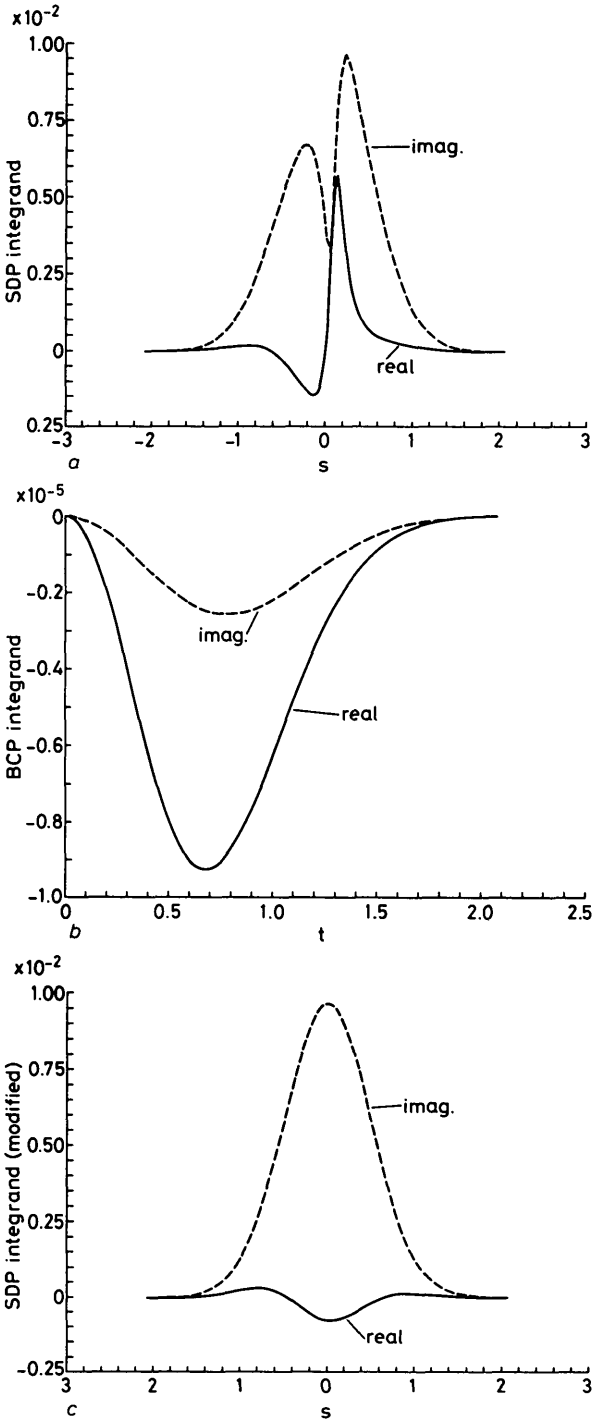

Fig. 7 *Plot of the* ${}_0\Pi_{vz}$ *integrand (improved approach) for the parameters of Fig. 4*

a SDP integrand
b BCP integrand
c Modified SDP integrand (Zenneck pole subtracted)

Table 1: Sample values of ${}_0\Pi_{vz}^{SDP}$, ${}_0\Pi_{vz}^{BCP}$, and ${}_0\Pi_{vz}$

		Rahmat-Samii *et al.* [2, 5]	Improved method
$f = 10$ MHz $\varepsilon = 10$ $\sigma = 2 \cdot 10^{-4}$ S/m $\theta_2 = 78°$ $r_2 = 1$ m	SDP	$1.2587 \cdot 10^{-1} - j3.1269 \cdot 10^{-2}$	$1.4283 \cdot 10^{-1} - j4.4775 \cdot 10^{-2}$
	BCP	$1.2524 \cdot 10^{-2} - j6.6071 \cdot 10^{-3}$	$-4.4418 \cdot 10^{-3} + j6.8982 \cdot 10^{-3}$
	Total	$1.3839 \cdot 10^{-1} - j3.7877 \cdot 10^{-2}$	$1.3839 \cdot 10^{-1} - j3.7877 \cdot 10^{-2}$
$f = 100$ MHz $\varepsilon = 80$ $\sigma = 1 \cdot 10^{-2}$ S/m $\theta_2 = 85°$ $r_2 = 1$ m	SDP	$-8.4103 \cdot 10^{-2} - j1.1116 \cdot 10^{-1}$	$-8.4707 \cdot 10^{-2} - j1.1141 \cdot 10^{-1}$
	BCP	$-6.1223 \cdot 10^{-4} - j2.2608 \cdot 10^{-4}$	$-7.5064 \cdot 10^{-6} + j1.5079 \cdot 10^{-5}$
	Total	$-8.4715 \cdot 10^{-2} - j1.1139 \cdot 10^{-1}$	$-8.4714 \cdot 10^{-2} - j1.1139 \cdot 10^{-1}$

noted that the SDP integrands are continuous and the BCP integrands are smooth and rapidly decaying. The values of the BCP and SDP integrals are given in Table 1 for the two examples. It is observed that, although the values of the particular integrals are different in the two techniques, the total values are the same, as expected (the small differences are due to numerical noise). These results also show that the values of the BCP integrals in the proposed method are one order of magnitude smaller than the corresponding values in the Rahmat-Samii *et al.* technique. Therefore, the branch-cut integrals are most likely to be negligible in comparison to the SDP integrals in the present method.

Although the SDP integrands in the modified approach are continuous, they still exhibit a rapid variation near $s = 0$, which is due to the Zenneck pole [2, 5]

$$\xi_z = \frac{\pi}{2} + j\{\mathrm{Ln}\,(\sqrt{\kappa} - j) - \mathrm{Ln}\,(\sqrt{\kappa} + 1)\} \tag{37}$$

In the complex s-plane, which is defined by the transformation of eqn. 11, this pole is located at

$$s_z = e^{-j(\pi/4)} \sqrt{1 + \frac{\cos\theta_2}{\sqrt{\kappa}+1} - \frac{\sqrt{\kappa}\sin\theta_2}{\sqrt{\kappa}+1}} \tag{38}$$

Although the Zenneck pole is never captured in the path deformation, it can get very close to the SDP when both the source and the field point are close to the interface and when the contrast between the media is large (Fig. 5). To remedy this, the Zenneck pole is subtracted from the SDP integrands of ${}_0\Pi_{vz}$ and ${}_0\Pi_{hz}$, rendering them slowly varying. Subsequently, the integrals of the subtracted terms are expressed in terms of the error function and added to the modified integrals to preserve their correct value. As a result of these steps, which closely follow the modified saddle-point procedure [8–10], one obtains

$${}_0\Pi_{vz}^{SDP} = \frac{k_1\kappa}{4\pi j} e^{-jk_1r_2} \left\{ \int_{-\infty}^{\infty} \left(P(\xi_{SDP})\alpha(s) - \frac{R_P}{s - s_z} \right) \times e^{-k_1r_2s^2}\, ds - j\pi R_P\, w(-\sqrt{k_1r_2}\, s_z) \right\} \tag{39}$$

and

$${}_0\Pi_{hz}^{SDP} = -\frac{k_1}{4\pi} \cos\phi_2\, e^{-jk_1r_2} \times \left\{ \int_{-\infty}^{\infty} \left(T(\xi_{SDP})\alpha(s) - \frac{R_T}{s - s_z} \right) e^{-k_1r_2s^2}\, ds - j\pi R_T\, w(-\sqrt{k_1r_2}\, s_z) \right\} \tag{40}$$

where the residues R_P and R_T are given by

$$R_P = -\frac{\sqrt{\kappa}}{(\kappa - 1)\sqrt{\kappa} + 1} Q_0(\xi_z) \tag{41}$$

and

$$R_T = -\frac{\kappa}{(\kappa - 1)\sqrt{\kappa} + 1} Q_1(\xi_z) \tag{42}$$

with

$$Q_i(\xi_z) = -\frac{\sqrt{\kappa}}{(\kappa + 1)} H_i^{(2)}\left(k_1r_2 \sqrt{\frac{\kappa}{\kappa+1}} \sin\theta_2 \right) \times e^{jk_1r_2\sqrt{(\kappa/\kappa+1)}\sin\theta_2} \tag{43}$$

The function $w(\cdot)$ in eqns. 39–40 is the error function defined in Reference 11.

As an illustration, the modified integrand of eqn. 39 is plotted in Figs. 6*c* and 7*c* for the two cases considered before. It is observed that the sharp peaks present in Figs. 6*a* and 7*a* are completely removed. In Table 2 are shown the values of the modified integral in eqn. 39 and the values of the correction term containing the error function for the two examples (the term preceding the bracket in eqn. 39 has been included in these values).

Table 2: Sample values of the modified integral and the correction term in eqn. 39

$f = 10$ MHz $\varepsilon = 10$ $\sigma = 2 \cdot 10^{-4}$ S/m $\theta_2 = 78°$ $r_2 = 1$ m	Modified integral	$1.5844.10^{-1} - j3.1193 \cdot 10^{-2}$
	Correction	$1.5605 \cdot 10^{-2} + j1.3581 \cdot 10^{-2}$
	Total	$1.4283 \cdot 10^{-1} - j4.4775 \cdot 10^{-2}$
$f = 100$ MHz $\varepsilon = 80$ $\sigma = 1 \cdot 10^{-2}$ S/m $\theta_2 = 85°$ $r_2 = 1$ m	Modified integral	$-7.9890 \cdot 10^{-2} - j1.3813 \cdot 10^{-1}$
	Correction	$4.8167 \cdot 10^{-3} - j2.6720 \cdot 10^{-2}$
	Total	$-8.4707 \cdot 10^{-2} - j1.1141 \cdot 10^{-1}$

5 Summary and conclusions

A modification of the Rahmat-Samii *et al.* technique for the numerical evaluation of Sommerfeld integrals has been described. The modified method differs from the original one in a computationally more efficient treatment of both the steepest-descent path (SDP) and the branch-cut path (BCP) integrals. The gain in efficiency is achieved by (i) letting the SDP enter the bottom sheet, which removes the discontinuity of the integrands; (ii) deforming the fundamental branch cut to the steepest-descent path from the branch point, which results in smooth and rapidly decaying integrands; (iii) subtracting the Zenneck pole from the SDP integrands, which renders them slowly varying; and (iv) by eliminating the need of solving a nonlinear equation to determine the point of intersection of the SDP with the BCP. It should be pointed out, however, that the advantages of the improved technique are significant only in cases when the BCP integral is not negligible in comparison with the SDP integral (small losses), and when the Zenneck pole occurs close to the SDP (high media contrast, source and field points close to the interface).

As a result of the improvements mentioned above, the integrands on both the SDP and the BCP are well behaved and low-order Gaussian quadratures can be employed for a much broader range of parameters than in the Rahmat-Samii *et al.* approach. It is found that in most cases a 32-point rule is sufficient on the SDP, and a 16-point rule on the BCP. In contrast to some other techniques, the present approach is efficient for both the near-field and the far-field computation. The effective integration intervals contain relatively few oscillations of the integrands, which is an advantage over the approach given in Reference 6. Also, the integrands do not exhibit sharp peaks, as is the case in the method given in Reference 7.

Unlike the original technique [2, 5], the improved method is fully consistent with the asymptotic techniques for approximate evaluation of integrals in terms of a large parameter [8–10]. Therefore, for large values of k_1r_2, the saddle-point method can be directly applied to eqns. 20

and 39–40, and the method of steepest descent can be used to approximately evaluate eqns. 30–32.

Finally, it is pointed out that this approach can, in principle, be applied in the case when the lower halfspace is replaced by a layered medium, such as the grounded dielectric slab, which is pertinent to microstrip antennas. However, the occurrence of the surface wave poles and the leaky wave poles, which may be exposed in the process of contour deformation, will make the application of this procedure much more difficult [12].

6 Acknowledgments

The author wishes to thank Professors Chalmers M. Butler and Charles E. Smith for their encouragement and interest in this work, and Dr. Yahya Rahmat-Samii for providing the subroutine for the computation of the error function of a complex argument.

This work was supported in part by the Committee on Faculty Research of the University of Mississippi.

7 References

1 SOMMERFELD, A.: 'Partial differential equations' (Academic Press, 1949), pp. 246–267

2 RAHMAT-SAMII, Y., MITTRA, R., and PARHAMI, P.: 'Evaluation of Sommerfeld integrals for lossy half-space problems', *Electromagnetics*, 1981, **1**, pp. 1–28

3 BURKE, G.J., MILLER, E.K., BRITTINGHAM, J.N., LAGER, D.L., LYTLE, R.J., and OKADA, J.T.: 'Computer modeling of antennas near the ground', *ibid.*, 1981, **1**, pp. 29–49

4 MOHSEN, A.: 'On the evaluation of Sommerfeld integrals', *IEE Proc. H, Microwaves, Opt. & Antennas*, 1982, **129**, pp. 177–182

5 PARHAMI, P., RAHMAT-SAMII, Y., and MITTRA, R.: 'An efficient approach for evaluating Sommerfeld integrals encountered in the problem of a current element radiating over lossy ground', *IEEE Trans.*, 1980, **AP-28**, pp. 100–104

6 JOHNSON, W.A., and DUDLEY, D.G.: 'Real axis integration of Sommerfeld integrals: source and observation points in air', *Radio Sci.*, 1983, **18**, pp. 175–186

7 LINDELL, I.V., and ALANEN, E.: 'Exact image theory for the Sommerfeld half-space problem, Part I: vertical magnetic dipole', *IEEE Trans.*, 1984, **AP-32**, pp. 126–133

8 FELSEN, L.B., and MARCUVITZ, N.: 'Radiation and scattering of waves' (Prentice-Hall, 1973)

9 BREKHOVSKIKH, L.M.: 'Waves in layered media' (Academic Press, 1980)

10 BERNARD, G.D., and ISHIMARU, A.: 'On complex waves', *Proc. IEE*, 1967, **114**, pp. 43–49

11 ABRAMOWITZ, M., and STEGUN, I.A. (Eds.): 'Handbook of mathematical functions' (Dover, 1965)

12 BLOK, H., VAN SPLUNTER, J.M., and JANSSEN, H.G.: 'Leaky-wave modes and their role in the numerical evaluation of the field excited by a line source in a non-symmetric, inhomogenously layered, slab waveguide'. Proc. International URSI Symposium, Universidad de Santiago de Compostela, Spain, 1983, pp. 523–526